Tempol-mediated activation of latent iron regulatory protein activity prevents symptoms of neurodegenerative disease in IRP2 knockout mice

Manik C. Ghosh*, Wing-Hang Tong*, Deliang Zhang*, Hayden Ollivierre-Wilson*, Anamika Singh*, Murali C. Krishna†, James B. Mitchell†, and Tracey A. Rouault*‡

*National Institute of Child Health and Human Development and †Radiation Biology Branch, Center for Cancer Research, National Cancer Institute, National Institutes of Health, Bethesda, MD 20892

Communicated by Richard D. Klausner, The Column Group, Seattle, WA, June 5, 2008 (received for review March 20, 2008)

In mammals, two homologous cytosolic regulatory proteins, iron regulatory protein 1 (also known as IRP1 and Aco1) and iron regulatory protein 2 (also known as IRP2 and Ireb2), sense cytosolic iron levels and posttranscriptionally regulate iron metabolism genes, including transferrin receptor 1 (TfR1) and ferritin H and L subunits, by binding to iron-responsive elements (IREs) within target transcripts. Mice that lack IRP2 develop microcytic anemia and neurodegeneration associated with functional cellular iron depletion caused by low TfR1 and high ferritin expression. IRP1 knockout (IRP1$^{-/-}$) animals do not significantly misregulate iron metabolism, partly because IRP1 is an iron-sulfur protein that functions mainly as a cytosolic aconitase in mammalian tissues and IRP2 activity increases to compensate for loss of the IRE binding form of IRP1. The neurodegenerative disease of IRP2$^{-/-}$ animals progresses slowly as the animals age. In this study, we fed IRP2$^{-/-}$ mice a diet supplemented with a stable nitroxide, Tempol, and showed that the progression of neuromuscular impairment was markedly attenuated. In cell lines derived from IRP2$^{-/-}$ animals, and in the cerebellum, brainstem, and forebrain of animals maintained on the Tempol diet, IRP1 was converted from a cytosolic aconitase to an IRE binding protein that stabilized the TfR1 transcript and repressed ferritin synthesis. We suggest that Tempol protected IRP2$^{-/-}$ mice by disassembling the cytosolic iron-sulfur cluster of IRP1 and activating IRE binding activity, which stabilized the TfR1 transcript, repressed ferritin synthesis, and partially restored normal cellular iron homeostasis in the brain.

anemia | axonopathy | ferritin | iron-sulfur cluster | transferrin receptor

Iron regulatory proteins (IRPs) regulate cellular iron homeostasis by binding to RNA stem-loops known as iron-responsive elements (IREs) found within transcripts that encode iron metabolism proteins (reviewed in refs. 1 and 2). For instance, IRP binding to the IRE at the 5′end of ferritin H or L transcripts represses ferritin translation, whereas IRP binding to IREs in the 3′UTR of TfR1 and one isoform of the metal transporter DMT1 stabilizes the mRNA (3).

IRP1 is a bifunctional protein that alternates between two forms: In iron-replete cells, IRP1 contains a cubane iron–sulfur cluster and functions as a cytosolic aconitase that interconverts citrate and isocitrate (4), whereas upon loss of its redox-sensitive iron–sulfur cluster, IRP1 undergoes a significant conformational change that enables it to bind to IREs (5). In animal tissues, most IRP1 contains an intact iron-sulfur cluster and functions mainly as an active aconitase. IRP1$^{-/-}$ animals do not exhibit significant misregulation of iron metabolism, and thus far, no significant phenotypes attributable to loss of cytosolic aconitase have been identified (6).

In contrast, animals that lack IRP2 (IRP2$^{-/-}$) develop mild microcytic anemia (7, 8) and progressive adult-onset neurodegeneration, as evidenced by axonal degeneration in the central nervous system (9, 10) and compromise of motor capabilities revealed by diminished performance on the hang test (9, 10) and on the rotarod test (11). Although one group did not observe neuropathological changes (11), both groups that generated IRP2$^{-/-}$ mice reported significant impairments of motor ability using either the hang test or the rotarod, and both groups observed markedly decreased grooming activity in IRP2$^{-/-}$ mice (9, 11, 12). Ferritin levels are abnormally high in tissues of IRP2$^{-/-}$ animals, whereas TfR1 levels are abnormally low (6), and increased ferritin and decreased TfR1 levels are present in brain tissues (9, 11, 12). Notably, IRP2$^{-/-}$ animals that also lack one IRP1 allele show greater misregulation of IRP target transcripts along with increased severity of anemia and neurodegenerative disease, indicating that the small fraction of IRP1 that has IRE binding activity contributes to regulation of intracellular iron metabolism (10, 12). Consistent with the notion that the IRE binding activity of IRP1 is important in iron homeostasis, levels of IRP2 show a compensatory increase in cells and tissues of IRP1$^{-/-}$ animals (6, 13), and developing embryos that lack both alleles of IRP1 and IRP2 (IRP1$^{-/-}$ IRP2$^{-/-}$) do not survive beyond the blastocyst stage of development (14).

Because our previous studies indicated that IRP1$^{-/-}$ animals were able to maintain normal iron metabolism primarily because IRP2 compensated for the loss of IRP1 (6, 13), we have been puzzled as to why IRP1, which is abundant in most tissues, does not compensate for the loss of IRP2 by converting from the cytosolic aconitase form to the IRE binding form. Our previous studies indicated that the iron–sulfur cluster of IRP1 was relatively stable at the low oxygen concentrations of most mammalian tissues (13) and that IRP1 was much less sensitive to changes in the iron status of mammalian tissues than IRP2.

As the iron–sulfur cluster of IRP1 is subject to oxidative disassembly on exposure to nitric oxide donor compounds (15, 16), we asked whether treatment of animals with a diet supplemented with the stable nitroxide 4-hydroxy-2,2,6,6-tetramethylpiperidine-N-oxyl, known as Tempol (17), would have a positive impact on the neurodegenerative disease of IRP2$^{-/-}$ animals. Tempol has been used as a scavenger of free radicals in several mouse models, and dietary Tempol supplementation resulted in decreased risk of developing cancer in Atm mutant mice (18) and in Fanconi anemia mice (19). In IRP2$^{-/-}$ mice, we observed that progression of neuromuscular compromise was

Author contributions: M.C.G., W.-H.T., D.Z., M.C.K., J.B.M., and T.A.R. designed research; M.C.G., W.-H.T., D.Z., H.O.-W., and A.S. performed research; M.C.G., W.-H.T., D.Z., H.O.-W., M.C.K., and J.B.M. contributed new reagents/analytic tools; M.C.G., W.-H.T., D.Z., A.S., M.C.K., J.B.M., and T.A.R. analyzed data; and M.C.G. and T.A.R. wrote the paper.

The authors declare no conflict of interest.

Freely available online through the PNAS open access option.

‡To whom correspondence should be addressed at: Molecular Medicine Program, National Institute of Child Health and Human Development, Bethesda, MD 20892. E-mail: rouault@mail.nih.gov.

This article contains supporting information online at www.pnas.org/cgi/content/full/0805361105/DCSupplemental.

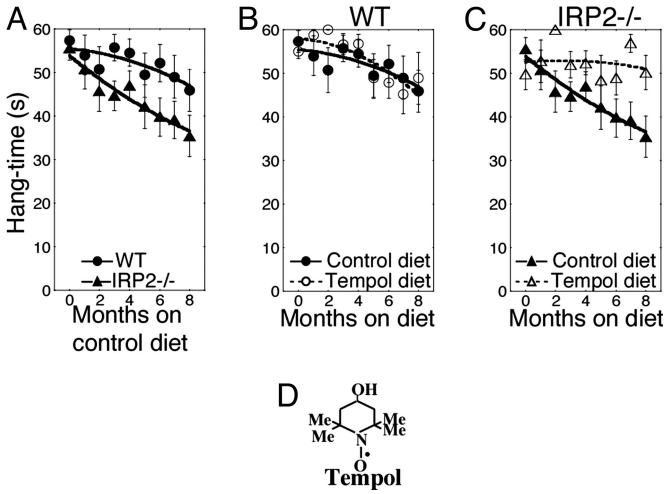

Fig. 1. Dietary Tempol supplementation prevents progressive neuromuscular deterioration in IRP2$^{-/-}$ mice. (*A*) Hang test studies on cohorts of WILD-TYPE and IRP2$^{-/-}$ animals revealed progressive neuromuscular compromise of IRP2$^{-/-}$ animals (n = 22) compared with wild type (n = 22) for animals maintained on the control diet (see *Materials and Methods*). (*B*) Hang test results from wild-type animals on a control (n = 22) or Tempol-supplemented diet (n = 22). (*C*) IRP2$^{-/-}$ animals on a diet supplemented with Tempol (n = 22) markedly improved their performance on the hang test compared with the animals on the control diet (n = 22). (*D*) The structure of Tempol is shown. Error bars represent standard error of the mean. The curves were drawn by using the polynomial curve fit of the KaleidaGraph program (Synergy).

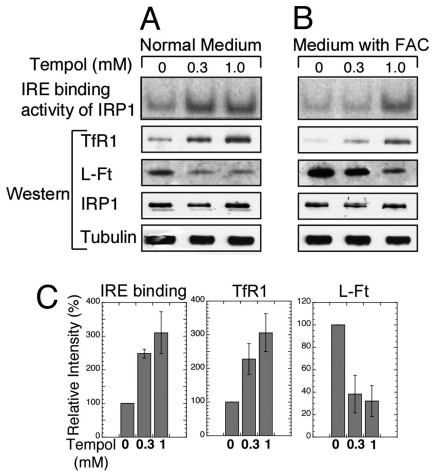

Fig. 2. Tempol supplementation activated the IRE binding activity of IRP1, increased TfR1 levels, and decreased ferritin expression in mouse embryonic fibroblasts derived from IRP2$^{-/-}$ animals. (*A*) IRP2$^{-/-}$ embryonic fibroblasts were maintained in cultures supplemented with 0, 0.3, or 1.0 mM Tempol for 16 h. In cells that lacked IRP2, all IRE binding activity in the first row was attributable to IRP1 activation. Western blots revealed that TfR1 levels increased, and ferritin levels decreased in Tempol treated cells, whereas IRP1 and tubulin levels (loading control) did not significantly change. (*B*) IRP2$^{-/-}$ embryonic fibroblasts were maintained in cultures supplemented with 300 μM ferric ammonium citrate (FAC) and 0, 0.3, or 1.0 mM Tempol for 16 h. Increased IRE binding activity of IRP1 correlated with increased TfR1 levels and decreased ferritin levels. (*C*) IRE binding activities of IRP1 and TfR1 and L-Ft protein levels in the absence and presence of two different concentrations of Tempol without added FAC were quantified in comparison with the intensity of the control lanes, represented as 100%. Error bars represent the standard deviation calculated from the results of two different sets of experiments.

markedly diminished in animals maintained on a Tempol-supplemented diet compared with IRP2$^{-/-}$ animals maintained on an unsupplemented diet. However, unlike the other mouse models in which Tempol has been therapeutically effective, we could not find evidence for free radical damage in IRP2$^{-/-}$ mice. Instead, we observed that IRP1 was converted from the aconitase to the IRE binding form in extracts from the cerebellum, forebrain, and brainstem of mice maintained on a Tempol-supplemented diet. We suggest that Tempol treatment prevented progression of symptoms in IRP2$^{-/-}$ mice because it activated the latent IRE binding activity of IRP1 and thereby allowed restoration of normal iron homeostasis in the central nervous system.

Results and Discussion

The neurodegeneration of IRP2$^{-/-}$ mice is characterized by progressive loss of motor capabilities, as measured by performance on hang tests (9, 10) and rotarod testing (11), decreased grooming activities (9, 11), and gait abnormalities in adult animals (9, 10). To quantitatively assess the progression of neurodegeneration, we used the hang test, which gauges the severity of neuromuscular compromise by measuring the length of time that a mouse can hang on to an inverted wire mesh before falling (up to a maximum of 60 sec) (20, 21). The hang test was performed at periodic intervals on cohorts of aging mice. The ability of IRP2$^{-/-}$ mice to maintain their grip after inversion of the wire mesh diminished progressively as animals grew older and was significantly worse (P = 0.015) in IRP2$^{-/-}$ mice compared with wild-type mice [Fig. 1*A* and supporting information (SI) Movie S1, a movie demonstration of the performance of wild-type and IRP2$^{-/-}$ mice on the hang test].

As the neurodegeneration of IRP2$^{-/-}$ animals progresses slowly in aging animals, we attempted to prevent disease progression by feeding wild-type, IRP2$^{-/-}$, and IRP1$^{+/-}$ IRP2$^{-/-}$ animals a diet supplemented with Tempol, a stable nitroxide that has been shown to have protective effects in ischemic stroke, cardiac reperfusion injury, and animal models of Parkinson's disease (22, 23). IRP2$^{-/-}$ mice fed a diet supplemented with Tempol did not develop the motor disorders, tremors, abnormalities of gait and grooming, or compromised performance on the hang test (Fig. 1*A*) characteristic of untreated aging IRP2$^{-/-}$ mice. Whereas the performance of wild-type mice on the hang test was not significantly affected by Tempol supplementation (Fig. 1*B*), the hang test results indicated that IRP2$^{-/-}$ mice maintained on a diet supplemented with Tempol were significantly (P = 0.009) protected from progressive loss of neuromuscular capability (Fig. 1*C*).

Although Tempol is generally assumed to function as a free radical scavenger that provides therapeutic benefit by alleviating oxidative stress (22), multiple assays for oxidative stress in our IRP2$^{-/-}$ animals, including lipid oxidation, DNA oxidation (8-hydroxyguanine assays), and protein oxidation assays did not indicate that oxidative stress had an important role in disease progression (data not shown). Because there was no evidence that radical scavenging accounted for the neuroprotective effect of Tempol on IRP2$^{-/-}$ mice, we then asked whether Tempol had a positive effect on activity and/or expression of iron metabolism genes, including IRP1, TfR1, and ferritin in IRP2-deficient cells. Notably, the IRE binding activity of IRP1 in IRP2$^{-/-}$ embryonic fibroblasts cultured in Tempol-supplemented media (300 μM or 1 mM) increased markedly with increased Tempol concentrations in cells grown in media that was not supplemented with additional iron (Fig. 2*A*, first row) or was supplemented with 300 μM ferric ammonium citrate (FAC) (Fig. 2*B*, first row). The total concentrations of Tempol achieved in the heart, adipose, brain, kidney, and blood of mice maintained on the Tempol-supplemented diet for 2 weeks were (in μM) 40.1 ± 22.6, 12.6 ± 3.7, 16.8 ± 8.1, 232.9 ± 59.9, and 91.9 ± 19.9, respectively. The increase in IRE binding activity correlated with increased TfR1 levels and decreased ferritin expression in cells grown in normal

NEUROSCIENCE

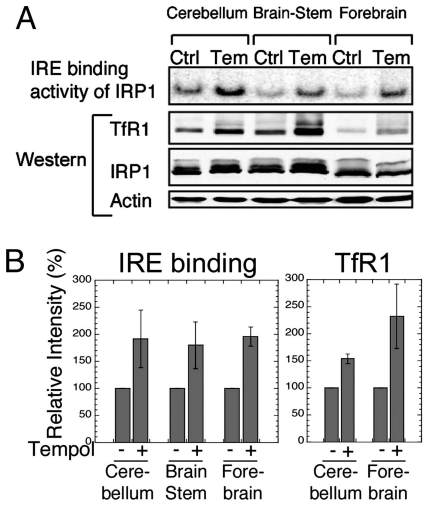

Fig. 3. IRE binding activity of IRP1 was increased in the brains of 11-mo-old IRP2$^{-/-}$ animals maintained for 10 mo on a Tempol-supplemented diet, resulting in increased expression of TfR1. (*A*) IRP2$^{-/-}$ animals on control (Ctrl) or Tempol (Tem) diets were killed, and lysates from the cerebellum, forebrain, and brain stem were analyzed by gel-shift assay and Western blot. IRE binding activity of IRP1 was increased by Tempol supplementation and TfR1 levels increased concomitantly, whereas total IRP1 and actin levels (loading control) did not change significantly after Tempol treatment. (*B*) IRE binding activities of IRP1 and TfR1 protein levels in different brain tissues from Tempol-supplemented mice were quantified relative to the intensity of the control mouse bands, represented as 100%. Error bars represent the standard deviation calculated from the results of two different sets of animals.

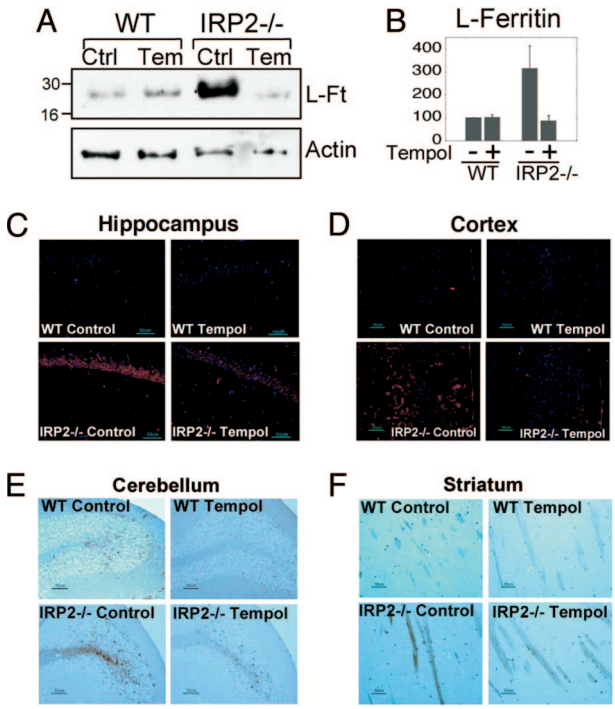

Fig. 4. Increased IRE binding activity induced by Tempol treatment leads to decreased ferritin expression in brain and reduced ferric iron accumulation in white matter. (*A*) Ferritin levels detected in Western blot of cerebellar lysates of wild-type animals on a control (Ctrl) (lane 1) or Tempol (Temp) diet (lane 2) compared with IRP2$^{-/-}$ animals on a control (lane 3) or Tempol diet (lane 4) indicated that increased cerebellar ferritin levels of untreated IRP2$^{-/-}$ animals were markedly reduced by treatment with Tempol. (*B*) L-Ft protein levels in the cerebellum from IRP2$^{-/-}$ mice on a control diet and Tempol-supplemented wild-type and IRP2$^{-/-}$ mice were quantified relative to the intensity of the wild-type control mouse bands, represented as 100%. Error bars represent the standard deviation calculated from the results of three different sets of animals. (*C*) Ferritin immunohistochemistry performed on animals on control diets revealed marked increases in ferritin expression in hippocampal neurons in IRP2$^{-/-}$ animals (*Lower Left*), which decreased with Tempol treatment (*Lower Right*). (*D*) Tempol treatment diminished ferritin overexpression in the cortex of IRP2$^{-/-}$ mice. (*E*) Cerebellar folia from wild-type and IRP2$^{-/-}$ animals were stained with Perls' DAB stain for detection of ferric iron. Ferric-iron staining increased in the white matter of IRP2$^{-/-}$ animals on a control diet compared with wild-type controls, but decreased in IRP2$^{-/-}$ animals on the Tempol diet. (*F*) Ferric-iron staining was also increased in the striatum of IRP2$^{-/-}$ animals but diminished in IRP2$^{-/-}$ animals on Tempol supplementation.

media with the indicated Tempol additions (Fig. 2*A*) and in media supplemented with FAC and Tempol (Fig. 2*B*) and occurred without significant changes in IRP1 protein levels (Fig. 2 *A* and *B*). Tempol-induced increases in IRE binding activity and TfR1 levels and decreases in L-ferritin (L-Ft) levels were significant and reproducible (Fig. 2*C*). Taken together, these results suggested that Tempol treatment allowed cells to compensate for the loss of IRP2 by activating the latent IRE binding activity of IRP1, thus reversing the misregulation of TfR1 and ferritin.

To determine whether Tempol increased the IRE binding activity of IRP1 *in vivo*, we compared the IRE binding activity of IRP1 in lysates made from various brain regions of IRP2$^{-/-}$ animals that were either maintained on a control diet or on the same diet supplemented with Tempol. In lysates from the cerebellum, brain stem, and forebrain, IRE binding activity markedly increased in Tempol-supplemented mice (Fig. 3 *A*, top row, and *B Left*). Furthermore, TfR1 protein levels also increased substantially, as expected when IRE binding activity increases, whereas IRP1 levels did not significantly change in the same brain regions (Fig. 3 *A* and *B*). Consistent with the observed increase of IRE binding activity induced by Tempol, ferritin levels decreased in the brains of IRP2$^{-/-}$ animals fed a diet supplemented with Tempol. In IRP2$^{-/-}$ animals maintained on the Tempol diet, ferritin levels decreased markedly in cerebellar lysates, whereas ferritin levels did not significantly change in wild-type mice on the Tempol-supplemented diet (Fig. 4 *A* and *B*). In addition, immunohistochemical analyses of mice on the Tempol diet demonstrated that ferritin expression decreased in the hippocampus (Fig. 4*C*) and cortex (Fig. 4*D*) of IRP2$^{-/-}$ mice. As reported (9, 10), increased ferritin expression correlated with increased ferric iron sequestration in oligodendrocytes and in the cerebellar white matter tracts of IRP2$^{-/-}$ animals. Notably, IRP2$^{-/-}$ animals maintained on the Tempol diet had less detectable ferric iron than those on a control diet, as determined by the enhanced Perls' 3,3′-diaminobenzidine (DAB) stain on the cerebellar folia and striatal regions of the brain (Fig. 4 *E* and *F*).

The increase in the IRE binding activity of IRP1 occurred without significant changes in IRP1 protein levels (Fig. 2), suggesting that Tempol treatment promoted disassembly of the iron–sulfur cluster of cytosolic aconitase to generate the IRE binding form of IRP1. To assess the status of the iron–sulfur cluster of IRP1, we performed in-gel aconitase assays to determine whether Tempol decreased the activity of cytosolic aconitase (24). The band that represented the cytosolic aconitase in mouse embryonic fibroblasts was readily identified by its absence in lysates from IRP1$^{-/-}$ cells (Fig. 5*A*). To further demonstrate the specificity of the in-gel aconitase assay, examples of this assay from mouse tissues and cells are shown in Fig. S1. Notably, Tempol treatment diminished the activity of cytosolic aconitase in lysates from wild-type and IRP2$^{-/-}$ embryonic fibroblasts (Fig. 5*A*), consistent with previous observations that small redox molecules, such as nitric oxide, O_2^-, and ascorbate, can react with

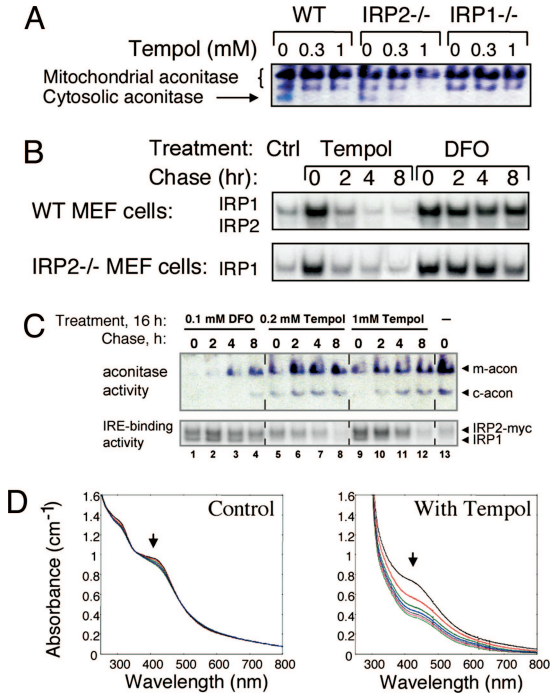

Fig. 5. Tempol treatment activates IRP1 to bind IREs by converting IRP1 from its cytosolic aconitase form to the IRE binding form. (*A*) The cytosolic aconitase activity in mouse embryonic fibroblast (MEF) lysates (arrow), as assessed in the in-gel aconitase assay for mouse lysates, was identified by its absence in IRP1$^{-/-}$ cells and was diminished by Tempol treatment of cells, as observed in lanes 2, 3, 5, and 6. (*B*) MEFs from wild-type or IRP2$^{-/-}$ animals were treated with 1.0 mM Tempol or 0.1 mM DFO for 16 h, after which they were switched to fresh unsupplemented media and assayed at various time points with gel-shift and aconitase gel assays. Recovery of aconitase activity was assessed in wild-type and IRP2$^{-/-}$ cells. (*C*) Aconitase activity (*Upper*) and IRE binding activity (*Lower*) of a HEK cell line engineered to overexpress *myc*-tagged IRP2 was assessed after 16 h treatments with media alone (lane 1), 0.1 mM DFO (lanes 2–6), 0.2 mM Tempol (lanes 6–9), or 1 mM Tempol (lanes 10–13). (*D*) Tempol degrades a purified synthetic [4Fe–4S] cluster. Repetitive spectral scanning of ≈60 μM solution of $(Bu_4N)_2[Fe_4S_4(SEt)_4]$ in acetonitrile maintained under anaerobic conditions over 140 min at 20-min intervals revealed minimal changes in the absorption profile (*Left*). Repetitive spectral scanning at 20-min intervals of ≈60 μM solution of $(Bu_4N)_2[Fe_4S_4(SEt)_4]$ to which a 9 mM solution of Tempol in acetonitrile was added demonstrated loss of characteristic absorption of the iron–sulfur cluster at 298 nm and 420 nm (*Right*).

the iron–sulfur cluster of the cytosolic aconitase, leading to loss of the iron–sulfur cluster and conversion to the IRE binding form of IRP1 (15, 16). Also, in mouse embryonic fibroblasts, mitochondrial aconitase activity was much less affected, consistent with reports that access of Tempol to mitochondria is relatively restricted, whereas modification of Tempol by conjugation of a lipophilic cation forms a compound, MitoTempol, that has greater access to mitochondria (25).

To determine whether the effect of Tempol on IRP1 activity was kinetically consistent with oxidative disassembly of the iron–sulfur cluster, we compared the effects of Tempol to those of the iron chelator deferoxamine mesylate (DFO), which activates IRE binding activity of IRP1 by limiting *de novo* synthesis and repair of the iron-sulfur cluster in IRP1. Both Tempol and DFO activated the IRE binding activity of IRP1 in mouse embryonic fibroblasts (Fig. 5*B*) and in a human embryonic kidney (HEK) cell line that overexpresses *myc*-tagged IRP2 (26) (Fig. 5*C*) after 16 h treatments. However, the activation of IRE binding activity and loss of cytosolic aconitase activity in human cell lines induced by Tempol was readily reversed within 2–4 h after removal of Tempol (Fig. 5*C Upper*, lanes 7 and 11), whereas little recovery of cytosolic aconitase activity was discernible even when activity was assessed 8 h after removal of DFO (Fig. 5*C Upper*, lane 4). The difference in the rate of iron–sulfur-cluster recovery indicated that Tempol and DFO activated IRP1 by distinct mechanisms. The slower recovery of aconitase activity in DFO-treated cells supports the notion that the iron–sulfur cluster of IRP1 was disassembled by Tempol but was readily rebuilt when the cluster destabilizing reagent was removed, whereas recovery of cytosolic aconitase activity after DFO treatment was limited by depletion of intracellular iron and reduced expression of iron-sulfur assembly proteins (24). Unlike what was observed in mouse embryonic fibroblasts, Tempol treatment also diminished (but did not abolish) mitochondrial aconitase activity in the HEK cell line. As observed in Fig. 5*C*, Tempol also increased expression of IRP2, an observation that is a subject of ongoing studies but is not relevant to treatment of mice that lack IRP2.

To assess whether the effect of Tempol on the iron–sulfur cluster status of IRP1 likely represents a direct chemical disassembly process, we analyzed the effects of Tempol on a synthetic iron–sulfur compound, $(Bu_4N)_2[Fe_4S_4(SEt)_4]$ (27), which contains a [4Fe–4S] cluster that absorbs UV light at 298 nm and visible light at 420 nm. Absorption of the intact iron–sulfur cluster diminished significantly in the sample treated with Tempol, whereas the sample treated with the addition of solvent alone showed little loss of its iron–sulfur cluster (Fig. 5*D*). Thus, our experiments demonstrated that Tempol readily degrades a generic [4Fe–4S] cluster. We therefore infer that Tempol activates IRE binding activity of IRP1 in cells and animals by directly destabilizing the [4Fe–4S] iron-sulfur cluster of IRP1, analogous to previous experiments with nitric oxide (28, 29).

Thus, it appears that Tempol protects IRP2$^{-/-}$ animals from progression of neuromuscular compromise by activating latent IRE binding activity of IRP1, which partially compensates for the loss of IRP2 by increasing TfR1 expression, decreasing ferritin expression, and improving iron homeostasis in the central nervous system of IRP2$^{-/-}$ animals. Even though there is no reproducibly measurable decrease in brain non-heme iron levels (data not shown), it is likely that functional iron deficiency because of loss of TfR1 and sequestration of iron within ferritin is a major cause of compromise in the central nervous system of IRP2$^{-/-}$ mice. Because ferric iron levels appear to be increased on iron stains, likely because of oxidation and sequestration by ferritin, whereas total non-heme iron levels are not significantly changed, it is likely that levels of bioavailable ferrous iron are decreased. Functional iron deficiency may be a major cause of the characteristic pathology of IRP2$^{-/-}$ mice, including axonal degeneration in numerous areas of the central nervous system (30).

Although Tempol treatment prevented symptoms of neurodegeneration, treatment with Tempol did not lead to an improvement in the mild anemia of IRP2$^{-/-}$ mice that likely resulted from decreased expression of TfR1 in erythroblasts and decreased bone marrow iron stores (7). The mild anemia of IRP2$^{-/-}$ mice (hematocrit was 46 ± 5 compared with 52 ± 2 for wild type, $P = 0.022$) did not improve in animals treated with Tempol (hematocrit 46 ± 4 after 8 mo of Tempol diet). To understand why Tempol would fail to correct the iron insufficiency anemia of IRP2$^{-/-}$ mice, we isolated erythroblasts from wild-type animals to assess the relative activities of IRP1 and IRP2 and to determine whether IRP1 could be recruited to the IRE binding form from a latent pool of IRP1 in erythroblasts. IRP1 levels were markedly lower in erythroblasts compared with brain (Fig. 6*B*). Gel-shift studies indicated that IRP1 and IRP2 equally contributed to IRE binding activity in erythroblasts (Fig. 6*A*). However, treatment of erythroblasts with high concentrations of β-mercaptoethanol (2%), which converts IRP1 from the cytosolic aconitase form to the IRE binding form, did not activate additional IRE binding activity of IRP1 in erythroblasts. In contrast, significant increases of IRE binding activity were recruited from brain lysates using β-mercaptoethanol treatment

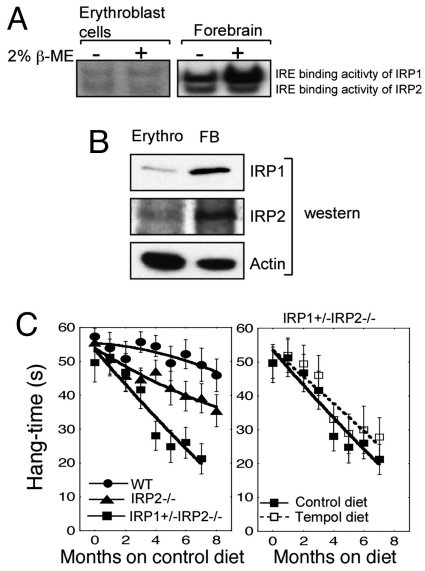

Fig. 6. Restoration of normal iron homeostasis by Tempol treatment depends on conversion of sufficient amounts of IRP1 to the IRE binding form. (*A*) Gel-shift studies demonstrate that erythoblast lysates contain little IRP1 that can be converted to the IRE binding form by treatment with 2% 2-mercaptoethanol, whereas forebrain lysates contain large amounts of IRP1 that can be recruited to bind IREs. Twenty micrograms of total protein was loaded in each lane. (*B*) Lysates from erythroblasts and forebrain indicate that IRP1 and IRP2 levels are low in erythroblasts (Erythro) compared with forebrain (FB). Twenty micrograms of total protein was loaded in each lane. (*C*) Hang test results of wild-type ($n = 22$), IRP2$^{-/-}$ ($n = 22$), and IRP1$^{+/-}$ IRP2$^{-/-}$ ($n = 6$) animals indicate that IRP1$^{+/-}$ IRP2$^{-/-}$ animals are more symptomatic than IRP2$^{-/-}$ animals [hang test curves of wild-type and IRP2$^{-/-}$ mice shown in Fig. 1 are redisplayed for comparison with IRP1$^{+/-}$ IRP2$^{-/-}$ animals (*Left*)]. However, Tempol treatment did not protect IRP1$^{+/-}$ IRP2$^{-/-}$ animals significantly ($P = 0.559$) from progression of neuromuscular compromise (*Right*). Error bars represent standard error of the mean. The curves were drawn by using the polynomial curve fit of the KaleidaGraph program.

(Fig. 6*A*), indicating that developing red cells lack a significant amount of IRP1 in the cytosolic aconitase form that can be converted to the IRE binding form by treatment with Tempol. Thus, Tempol did not correct the anemia of IRP2$^{-/-}$ mice because very little IRE binding activity could be recruited in erythroblasts.

Interestingly, because Tempol treatment prevented progressive motor compromise of the IRP2$^{-/-}$ animals (Fig. 1*C*), we asked whether Tempol treatment could also prevent progression of the disease of IRP1$^{+/-}$ IRP2$^{-/-}$ mice. As demonstrated, IRP1$^{+/-}$ IRP2$^{-/-}$ mice have even more pronounced axonal degeneration (10) and clinical compromise than IRP2$^{-/-}$ mice (Fig. 6*C Left*). Because IRP1$^{+/-}$ IRP2$^{-/-}$ mice have only one IRP1 allele, the IRP1$^{+/-}$ IRP2$^{-/-}$ animals would be expected to have only half the amount of IRP1 that could be activated by Tempol compared with the IRP2$^{-/-}$ mice. Tempol treatment did not significantly ($P = 0.559$) prevent disease progression in the IRP1$^{+/-}$ IRP2$^{-/-}$ mice (Fig. 6*C Right*), further supporting the notion that Tempol protects IRP2$^{-/-}$ mice by recruiting the latent IRE binding activity of IRP1. The observation that Tempol-dependent activation of the IRE binding activity of IRP1 correlates with neuroprotection of IRP2$^{-/-}$ mice further underscores the inference that neurodegeneration in IRP2$^{-/-}$ mice results from loss of total IRE binding activity (1, 9, 11, 12).

Tempol is an attractive potential neuroprotective treatment because it activates IRP1 by a mechanism that does not cause significant free radical stress or iron depletion; in addition, Tempol treatment of control animals did not cause observable side effects and was therefore relatively benign compared with other reagents that could be used to recruit IRE binding activity. Tempol is currently being evaluated for use in humans as a radioprotective reagent (31). Although human patients with IRP2 deficiency have not yet been identified, we suggest that humans with IRP2 deficiency would be expected to have adult-onset neurodegenerative disease (32) and IRP2 should be evaluated in patients with Parkinson's disease, multiple system atrophy, or amyotrophic lateral sclerosis, who have mild microcytic anemia, elevated serum ferritin, and elevated levels of protoporphyrin IX in red cells. Notably, human IRP2 is located within a small genomic region implicated in the development of lung cancer (33). The current study suggests that dietary Tempol would be effective against the progression of neurodegenerative diseases associated with IRP2 deficiency. Trials of neuroprotective agents in animal and human studies have been generally disappointing, perhaps because the underlying mechanisms of various forms of neurodegeneration are not well understood and animal models do not faithfully reflect human disease pathogenesis (34). In IRP2$^{-/-}$ animals, our understanding of pathogenesis and function has permitted critical evaluation of a specific nontoxic agent that prevents symptomatic disease progression by activating the latent activity of a duplicated gene to restore normal iron homeostasis in the brain.

Materials and Methods

Mice. IRP2$^{-/-}$ mice were generated, propagated by breeding, and genotyped (9) as described in *SI Materials and Methods*.

Chemicals. The synthetic [4Fe–4S] cluster $(Bu_4N)_2[Fe_4S_4(SEt)_4]$ (27) was a generous gift from Richard Holm and Tom Scott (Harvard University, Camridge, MA).

Diet Description. The mice were weaned at 3–4 wks of age. Immediately after weaning, mice were maintained on either the Tempol or control diet as described in *SI Materials and Methods*.

Assay of Tissue Tempol Concentrations. Female C3H/Hen mice at 9 wks of age were placed on a Tempol diet (10 mg of Tempol/g of food) (Bio-Serv). After 2 weeks on this diet, blood and tissue were collected and wet weight was determined for total Tempol concentration (35) as described in *SI Materials and Methods*.

Hang Test. The hang test was measured and recorded (20) as described in *SI Materials and Methods*.

Tissue and Lysate Preparation. Preparations of lysates for assays were performed anaerobically as described in *SI Materials and Methods*.

Cells. Embryonic fibroblasts (9), the *myc*-tagged HEK293 Tet-on cell line (26), and erythroblasts were prepared as described in ref. 7.

RNA Mobility Shift Assays. Gel retardation assays were performed (6) as described in *SI Materials and Methods*.

Western Blot Analysis and Antibodies. Protein analysis (9) was as described *SI Materials and Methods*.

Aconitase Assay. Aconitase activity gels for human lysates were performed as described in ref. 24 and with modifications, as described in *SI Materials and Methods*.

Spectrophotometric Study on the Effect of Tempol on a [4Fe–4S] Cluster. In an anaerobic chamber, solid $(Bu_4N)_2[Fe_4S_4(SEt)_4]$ (23) was dissolved in deaerated acetonitrile and assessed as described in *SI Materials and Methods*.

Immunohistochemistry and Perls' DAB Iron Staining. Procedures were performed (36) as described in *SI Materials and Methods*.

Statistics. We tested differences between means of hang-time by using a paired Student's *t* test. Results with $P < 0.05$ were considered statistically significant.

ACKNOWLEDGMENTS. We thank Sharon Cooperman, Kavitha Ramaswamy, and Michael Eckhaus for their help. This work was supported by the intramural programs of the National Institute of Child Health and Human Development and the National Cancer Institute.

1. Rouault TA (2006) The role of iron regulatory proteins in mammalian iron homeostasis and disease. *Nat Chem Biol* 2:406–414.
2. Wallander ML, Leibold EA, Eisenstein RS (2006) Molecular control of vertebrate iron homeostasis by iron regulatory proteins. *Biochim Biophys Acta* 1763:668–689.
3. Hentze MW, Muckenthaler MU, Andrews NC (2004) Balancing acts: Molecular control of mammalian iron metabolism. *Cell* 117:285–297.
4. Dupuy J, *et al.* (2006) Crystal structure of human iron regulatory protein 1 as cytosolic aconitase. *Structure* 14:129–139.
5. Walden WE, *et al.* (2006) Structure of dual function iron regulatory protein 1 complexed with ferritin IRE-RNA. *Science* 314:1903–1908.
6. Meyron-Holtz EG, *et al.* (2004) Genetic ablations of iron regulatory proteins 1 and 2 reveal why iron regulatory protein 2 dominates iron homeostasis. *EMBO J* 23:386–395.
7. Cooperman SS, *et al.* (2005) Microcytic anemia, erythropoietic protoporphyria, and neurodegeneration in mice with targeted deletion of iron-regulatory protein 2. *Blood* 106:1084–1091.
8. Galy B, *et al.* (2005) Altered body iron distribution and microcytosis in mice deficient in iron regulatory protein 2 (IRP2). *Blood* 106:2580–2589.
9. LaVaute T, *et al.* (2001) Targeted deletion of iron regulatory protein 2 causes misregulation of iron metabolism and neurodegenerative disease in mice. *Nat Genet* 27:209–214.
10. Smith SR, *et al.* (2004) Severity of neurodegeneration correlates with compromise of iron metabolism in mice with iron regulatory protein deficiencies. *Ann NY Acad Sci* 1012:65–83.
11. Galy B, *et al.* (2006) Iron homeostasis in the brain: Complete iron regulatory protein 2 deficiency without symptomatic neurodegeneration in the mouse. *Nat Genet* 38:967–969.
12. Ghosh MC, Ollivierre-Wilson H, Cooperman S, Rouault TA (2006) Reply to ''Iron homeostasis in the brain: Complete iron regulatory protein 2 deficiency without symptomatic neurodegeneration in the mouse.'' *Nat Genet* 38:969–970.
13. Meyron-Holtz EG, Ghosh MC, Rouault TA (2004) Mammalian tissue oxygen levels modulate iron-regulatory protein activities in vivo. *Science* 306:2087–2090.
14. Smith SR, Ghosh MC, Ollivierre-Wilson H, Hang Tong W, Rouault TA (2006) Complete loss of iron regulatory proteins 1 and 2 prevents viability of murine zygotes beyond the blastocyst stage of embryonic development. *Blood Cells Mol Dis* 36:283–287.
15. Pantopoulos K, Hentze MW (1995) Rapid responses to oxidative stress mediated by iron regulatory protein. *EMBO J* 14:2917–2924.
16. Bouton C, Drapier JC (2003) Iron regulatory proteins as NO signal transducers. *Sci STKE* 2003:pe17.
17. Mitchell JB, *et al.* (2003) A low molecular weight antioxidant decreases weight and lowers tumor incidence. *Free Radic Biol Med* 34:93–102.
18. Schubert R, *et al.* (2004) Cancer chemoprevention by the antioxidant tempol in Atm-deficient mice. *Hum Mol Genet* 13:1793–1802.
19. Zhang QS, *et al.* (2008) Tempol protects against oxidative damage and delays epithelial tumor onset in Fanconi anemia mice. *Cancer Res* 68:1601–1608.
20. Crawley JN (1999) Behavioral phenotyping of transgenic and knockout mice: Experimental design and evaluation of general health, sensory functions, motor abilities, and specific behavioral tests. *Brain Res* 835:18–26.
21. Liou YC, *et al.* (2003) Role of the prolyl isomerase Pin1 in protecting against age-dependent neurodegeneration. *Nature* 424:556–561.
22. Soule BP, *et al.* (2007) The chemistry and biology of nitroxide compounds. *Free Radic Biol Med* 42:1632–1650.
23. Hu G, Lyeth BG, Zhao X, Mitchell JB, Watson JC (2003) Neuroprotection by the stable nitroxide 3-carbamoyl-proxyl during reperfusion in a rat model of transient focal ischemia. *J Neurosurg* 98:393–396.
24. Tong WH, Rouault TA (2006) Functions of mitochondrial ISCU and cytosolic ISCU in mammalian iron-sulfur cluster biogenesis and iron homeostasis. *Cell Metab* 3:199–210.
25. Trnka J, Blaikie FH, Smith RA, Murphy MP (2008) A mitochondria-targeted nitroxide is reduced to its hydroxylamine by ubiquinol in mitochondria. *Free Radic Biol Med* 44:1406–1419.
26. Bourdon E, *et al.* (2003) The role of endogenous heme synthesis and degradation domain cysteines in cellular iron-dependent degradation of IRP2. *Blood Cells Mol Dis* 31:247–255.
27. DePamphilis BV, Averill BA, Herskovitz T, Que LJ, Holm RH (1974) Synthetic analogs of the active sites of iron-sulfur proteins. VI. Spectral and redox characteristics of the tetranuclear clusters (Fe4S4(SR)4). 2-. *J Am Chem Soc* 96:4159–4167.
28. Drapier JC, Hirling H, Wietzerbin J, Kaldy P, Kuhn LC (1993) Biosynthesis of nitric oxide activates iron regulatory factor in macrophages. *EMBO J* 12:3643–3649.
29. Soum E, Drapier JC (2003) Nitric oxide and peroxynitrite promote complete disruption of the [4Fe–4S] cluster of recombinant human iron regulatory protein 1. *J Biol Inorg Chem* 8:226–232.
30. Rouault TA, Cooperman S (2006) Brain iron metabolism. *Semin Pediatr Neurol* 13:142–148.
31. Metz JM, *et al.* (2004) A phase I study of topical Tempol for the prevention of alopecia induced by whole brain radiotherapy. *Clin Cancer Res* 10:6411–6417.
32. Coon KD, *et al.* (2006) Preliminary demonstration of an allelic association of the IREB2 gene with Alzheimer's disease. *J Alzheimers Dis* 9:225–233.
33. Hung RJ, *et al.* (2008) A susceptibility locus for lung cancer maps to nicotinic acetylcholine receptor subunit genes on 15q25. *Nature* 452:633–637.
34. Brew BJ (2007) Lost in translation: Again, another failed neuroprotection trial. *Neurology* 69:1308–1309.
35. Hyodo F, Matsumoto K, Matsumoto A, Mitchell JB, Krishna MC (2006) Probing the intracellular redox status of tumors with magnetic resonance imaging and redox-sensitive contrast agents. *Cancer Res* 66:9921–9928.
36. Zhang DL, Su D, Berczi A, Vargas A, Asard H (2006) An ascorbate-reducible cytochrome b561 is localized in macrophage lysosomes. *Biochim Biophys Acta* 1760:1903–1913.